miRNA repertoires of cystic fibrosis ex vivo models highlight miR-181a and miR -101 that regulate WISP1 expression

Alexandra Pommier, Jessica Varilh, Solenne Bleuse, Karine Délétang, Jennifer Bonini, Anne Bergougnoux, Emmanuelle Brochiero, Michel Koenig, Mireille Claustres, Magali Taulan-cadars

miRNA repertoires of cystic fibrosis *ex vivo* models highlight miR-181a and miR-101 that regulate WISP1 expression

Alexandra Pommier[1], Jessica Varilh[1], Solenne Bleuse[1], Karine Delétang[1], Jennifer Bonini[1], Anne Bergougnoux[1,2], Emmanuelle Brochiero[3,4], Michel Koenig[1,2], Mireille Claustres[1] and Magali Taulan-Cadars[1]*

[1] *Université de Montpellier, Laboratoire de Génétique de Maladies Rares EA7402, Montpellier, France*
[2] *CHU de Montpellier, Laboratoire de Génétique Moléculaire, Montpellier, France*
[3] *Centre de Recherche du Centre Hospitalier de l'Université de Montréal (CRCHUM), Montréal, QC, Canada*
[4] *Département de Médecine, Université de Montréal, Montréal, QC, Canada*

Correspondence to: M Taulan-Cadars, Laboratoire de Génétique de Maladies Rares, Institut Universitaire de Recherche Clinique, 641 Avenue du Doyen Gaston Giraud, 34093 Montpellier, France. E-mail: magali.taulan@inserm.fr

Abstract

Cystic fibrosis (CF), a genetic disorder, is characterized by chronic lung disease. Small non-coding RNAs are key regulators of gene expression and participate in various processes, which are dysregulated in CF; however, they remain poorly studied. Here, we determined the complete microRNAs (miRNAs) expression pattern in three CF *ex vivo* models. The miRNA profiles of air–liquid interface cultures of airway epithelia (bronchi, nasal cells, and nasal polyps) samples from patients with CF and non-CF controls were obtained by deep sequencing. Compared with non-CF controls, several miRNAs were deregulated in CF samples; for instance, miR-181a-5p and the miR-449 family were upregulated. Moreover, mature miRNAs often showed variations (i.e. isomiRs) relative to their reference sequence, such as miR-101, suggesting that miRNAs consist of heterogeneous repertoires of multiple isoforms with different effects on gene expression. Analysis of miR-181a-5p and miR-101-3p isomiRs indicated that they regulate the expression of WISP1, a key component of cell proliferation/migration programs. We showed that miR-101 and miR-181a-5p participated in aberrant recapitulation of wound healing programs by controlling WISP1 mRNA and protein level. Our miRNA expression data bring new insights into CF physiopathology and define new potential therapeutic targets in CF.

Keywords: miRNA; isomiR; cystic fibrosis; WISP1; wound healing; small RNAseq; miR-101; miR-181a; gene therapy; lung disease

Introduction

In cystic fibrosis (CF), the most common life-shortening genetic disorder in Caucasians, mutations of the *CFTR* gene, which encodes a chloride channel located at the apical membrane of epithelial cells, result in ion transport dysfunctions that contribute to impair mucociliary clearance, favoring bacterial colonization and inflammation, and ultimately leading to lung destruction. Small non-coding RNAs are key regulators of gene expression and contribute to various processes which are dysregulated in CF, including inflammation [1,2], but their precise role in this disease remains to be elucidated.

Mature microRNAs (miRNAs), a distinct class of small non-coding RNAs of 20–24 nucleotides in length, have been described in most animal species [3]. They regulate gene expression by binding to the target gene typically in the 3'-untranslated region (UTR) and then by modulating mRNA level and translation efficiency. Target recognition by miRNAs is based on the identification of specific sequences that are phylogenetically conserved. Importantly, in animals, a perfect match is required between the target site and 7–8 nucleotides at the miRNA 5'-end (a region known as 'seed', nucleotides 2–7 or 2–8). Nucleotides further downstream (nucleotides 13–16) can also contribute to base pairing with the mRNA target [4]. In animals, miRNA genes are transcribed into a primary miRNA (pri-miRNA) that is processed by the DROSHA enzyme to generate a precursor miRNA (pre-miRNA). This precursor is recognized by DICER and cut to obtain the mature miRNA. Moreover, miRNA variants, called isomiRs [5–7], are also generated following heterogeneous, i.e. imprecise, cleavage by DROSHA or/and DICER [8]. In these variants, the 'seed' sequence might be altered relative to the canonical miRNA, thus modifying the mRNA targets. Several studies have compared the miRNA expression profiles of CF IB3-1 and control IB3-1/S9 lung epithelial cells [9], CF and non-CF (NCF) bronchial brushing samples [10], and CF and NCF air–liquid interface (ALI)

airway epithelium cultures [11]. However, these data were obtained using TaqMan Low-Density microRNA Arrays (TLDAs), a sensitive targeted approach that allowed the quantification of only about 25% of all the existing miRNAs.

In this study, we used an exhaustive method (miRNA sequencing) to obtain the complete miRNA expression profile in three *ex vivo* CF models (ALI cultures derived from bronchial, nasal, and nasal polyp epithelium). We identified deregulated miRNAs in all three *ex vivo* models including miR-181a-5p and investigated their involvement in the regulation of the gene expression encoding factors of the PI3K–Akt and wound healing pathways, which are altered in CF [12,13]. We also identified several variants of isomiR-101 and tested their effect on the expression of several of its gene targets, including EZH2, CEBPA, and CFTR, on which we previously demonstrated its importance [14], and WISP1, a new target of miR-101-3p and miR-181a-5p. These data bring new insights into CF physiopathology and open new research opportunities in CF.

Materials and methods

Human airway epithelial cells

For human primary nasal polyp epithelial ALI cell cultures (ALI-polyps), primary cells from four healthy individuals (NCF) and four patients with CF (homozygous p.Phe508del in CFTR) were recovered after polypectomy and cultured, according to approved ethical protocols (Comité d'Ethique de la Recherche du CHUM) and with written informed consents at CHUM Hospital (Montréal, QC, Canada) [12,15].

Human nasal cells (ALI-nasal) from three patients with CF (homozygous p.Phe508del in CFTR) and three healthy donors (NCF) were cultured as previously described [14]. Human bronchial epithelial cells (ALI-bronchial) from lung tissues of NCF donors ($n = 5$) or patients with CF ($n = 5$), obtained during surgery, were purchased from Epithelix (Plan-Les-Ouates, Switzerland).

Primary normal and CF human airway epithelial cell lines (hAECB and hAECB-CF, respectively) of bronchial origin were purchased from Epithelix.

Immortalized human bronchial epithelial cell line BEAS-2B, 16HBE14o$^-$ cells (16HBE) and CFBE41o$^-$ (CFBE) derived from human normal or CF bronchi, respectively, were cultured. Details are provided in Supplementary materials and methods.

Small RNA sequencing, miRNA annotation, and differential expression

One microgram of total RNA with RNA integrity number (RIN) greater than 7 was used for library construction using a TruSeq Small RNA kit (Illumina®, San Diego, CA, USA). After size control validation using an Agilent 2100 Bioanalyzer (Agilent, Santa Clara, CA, USA), 12 small-RNA libraries were prepared and pooled together, and then sequenced at 12 pM using an MiSeq (Illumina®). In total, we prepared 24 libraries ($n = 5$ for NCF/CF bronchial ALI cells, $n = 4$ for NCF/CF nasal ALI cells, and $n = 3$ for NCF/CF polyp ALI cells). To annotate miRNAs and conduct differential expression, the FastQ files were analyzed using the sRNAbench webserver [16], which integrates sRNAde, a computational tool (v1.0) for differential expression analysis which is based on different algorithms including DESeq, edgeR, and NOIseq [17]. For high confidence results, a minimum readcount of 10 and a length between 18 and 26 nt were set.

Luciferase reporter assays

BEAS-2B (10 000 cells per well) were co-transfected with reporter constructs pGL3c-3'-UTR gene and miRNA (20 nM), isomiRs (20 nM), and miRNA inhibitors (100 nM) (see Supplementary materials and methods). All luciferase activities represent at least three independent experiments, with each construct tested in triplicate per experiment.

In vitro wound healing assays

16HBE and CFBE cell monolayers (seeded at 50 000 cells per well) were transfected with miRNA inhibitors and scratched using a sterile plastic micropipette P20 tip (for details see Supplementary materials and methods). Twenty-four hours after transfection, cells were then washed three times with PBS and medium to remove cell debris. Several areas were marked on the Petri dishes so that photographs could be taken at exactly the same places at defined times (0 and 24 h of wound closure). The wound closure rate was evaluated using microscopy images on a confocal Leica SP8-UV (Leica Microsystems, Wetzlar, Germany; ×20 objective enlargement) and images were processed using ImageJ software (NIH, Bethesda, MD, USA). For each condition, two independent experiments were produced for 16HBE cells and four independent experiments for CFBE cells. The ratio of wound closure healing corresponds to the wound closure for the treated condition versus the control condition.

Indirect immunofluorescence

16HBE and CFBE cells were transfected with inhibitors for 24 h and prepared as detailed in Supplementary materials and methods. In brief, the cells were incubated with anti-WISP1 (1:50) for 1 h, then with anti-mouse Alexa 647 conjugated secondary antibody (1:500) for 1 h, and counterstained with DAPI (1:5000) for 1 min.

Quantification of mRNAs and miRNAs

Total RNA was purified with TRIzol™ Reagent (Life Technologies SAS, Saint-Aubin, France). Reverse transcription (RT) was performed using 1 µg of total RNA

by using M-MLV reverse transcriptase (Fisher Scientific, Illkirch, France) or 40 ng of total RNA using a miRCURY LNA™ Universal cDNA Synthesis Kit (Exiqon, Vedbaek, Denmark) for mRNA or miRNA quantification, respectively. For both mRNAs and miRNAs, RT-qPCR was performed using a 1:10 dilution of cDNA on a Roche LC480 LightCycler instrument (Roche Diagnostics, Meylan, France) as described previously [14]. Relative expression of mRNAs and miRNAs of interest was determined using the 2(−ddCt) method.

mRNA expression by PCR array

Reverse transcription was performed using 400 ng of total RNA from ALI-bronchial cells (same samples used for small RNA sequencing) by using an RT^2 First Strand kit (Qiagen, Courtaboeuf, France) following the manufacturer's protocol. We used an RT^2 Profiler PCR Array (Qiagen) that focuses on genes for WNT signaling targets, wound healing, and PI3K–AKT signaling pathways; reactions were performed using a 1:5 dilution of first-strand cDNA. Relative expression levels were calculated using the comparative ΔΔCt method with five genes as endogenous controls (*ACTB*, *B2M*, *GAPDH*, *HPRT1*, *RPLP0*).

Western blotting

Proteins (25–50 µg) were electrophoresed through 7% (for CFTR proteins) or 10% (for other proteins) SDS polyacrylamide gels. After transfer and blocking steps, membranes were incubated overnight at 4 °C with primary antibodies (for details see Supplementary materials and methods).

Details of transient transfection assays and the statistical analyses used are provided in Supplementary materials and methods.

Results

miRNA expression profiles in ALI airway cell cultures

Genome-wide sequencing analysis of the miRNA expression profiles in NCF and CF ALI-polyp, ALI-nasal, and ALI-bronchial samples showed that, on average, 266 microRNAs were detected in each sample type and 179 had a readcount higher than 10 reads (Figure 1A). About 70% of reads mapped to human miRNAs (miRBase v21). Comparison of the expression of the top 20 miRNAs (on average, 80% of all expressed miRNAs) in NCF ALI-bronchial, ALI-polyp, and ALI-nasal samples indicated that they were similarly expressed in all three models, and particularly between ALI-polyp and ALI-nasal samples (Figure 1B). Then sRNAde, a computational tool integrated in the sRNA-bench webserver for differential expression analysis, was used to rank the miRNAs that were differentially expressed in CF and NCF samples. The correlation between miRNA expression in CF and NCF samples was consistent ($r^2 = 0.91$ and 0.92) (supplementary material, Figure S1). Filtering of the list of miRNAs with $p < 0.05$ between CF and NCF samples indicated the deregulation of 35, 68, and 50 miRNAs in CF ALI-bronchial, ALI-nasal, and ALI-polyp samples, respectively (Figure 1C). An additional filtering of the list of miRNAs with considered deregulated miRNAs with fold-change >2 or <0.5 between CF and NCF samples indicated that nine miRNAs were upregulated and 16 were downregulated in CF ALI-bronchial samples compared with NCF samples (Table 1). Moreover, 16 and 20 miRNAs were upregulated in CF ALI-nasal and ALI-polyp samples, respectively, and 23 and 11 were downregulated, respectively, compared with NCF controls (supplementary material, Tables S1 and S2). Among the dysregulated miRNAs, five were detected in all three models: miR-9-5p, miR-1246, miR-181a-5p, miR-181a-2-3p, and miR-10a-5p. miR-9-5p was strongly downregulated in CF ALI-bronchial and ALI-nasal cells (data confirmed by RT-qPCR; supplementary material, Figure S2A) and overexpressed in CF ALI-polyp cultures. miR-1246, miR-181a-5p, and miR-181a-2-3p were upregulated in CF ALI-bronchial and ALI-nasal cells, and downregulated in ALI-polyp samples. miR-10a-5p was overexpressed in CF ALI-nasal cells and downregulated in CF ALI-bronchial and ALI-polyp samples. Overall, ALI-nasal and ALI-bronchial miRNA profiles were the most similar (30% of deregulated miRNAs were the same in the two models).

miR-181a-5p targets the PI3K–AKT and wound healing pathways

TargetScan (http://www.targetscan.org/vert_72/), miRDB (http://www.mirdb.org/), and Diana tools microT-CDS (http://diana.imis.athena-innovation.gr/DianaTools/index.php?r=site/index) were used to build the list of genes predicted to be targeted by the miRNAs that were differentially expressed in CF cultures, and these data were integrated in DAVID (v6.8, Database for Annotation, Visualization and Integrated Discovery) bioinformatics resources. This analysis retained the same top ten pathways for all three models, particularly the PI3K–AKT pathway (Figure 2A). We chose to further investigate this pathway ($p = 0.0052$) because it contains numerous genes targeted by deregulated miRNA and it has been recently described in CF [13]. Targeted PCR array (Qiagen) analysis with 84 predesigned primer sets for assessing the expression of genes included in the PI3K–AKT pathway showed that in CF samples, four genes were downregulated (*AKT3*, *CD14*, *IGF1*, and *PIK3CG*) and two were upregulated (*PDGFRA* and *PRKCA*). Because some of the deregulated miRNAs targeted the wound healing pathway and related genes ($p = 0.0043$), a targeted PCR array was also employed. Among the 84 genes tested, six were upregulated (*CCL2*, *COL14A1*, *COL4A1*, *CXCL11*, *MMP1*, and *PLG*) and four were downregulated (*CTSL2*, *F13A1*, *IGF1*, and *WISP1*). These results were confirmed by RT-qPCR in CF bronchial epithelium using newly designed primers (data not shown). Among these

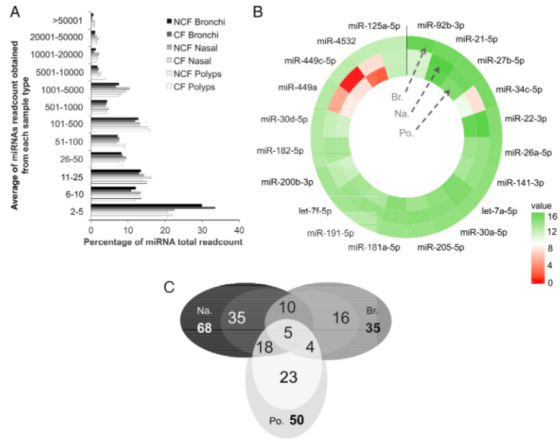

Figure 1. miRNA level in CF and NCF ALI cultures of airway epithelium obtained by miRNA sequencing. (A) Bar charts showing the distribution of miRNA total readcounts for each sample type (CF, cystic fibrosis; NCF, non-CF). As more than one million reads were obtained per sample, for each condition (NCF/CF ALI-bronchial, $n = 5$; NCF/CF ALI-nasal, $n = 3$; NCF/CF ALI-polyp samples, $n = 4$), the average percentage of miRNAs (*x*-axis) for each specific range of reads (sequencing depth) is shown. (B) Expression profiles of the 20 most expressed miRNAs in NCF ALI-bronchial (Br., $n = 5$), ALI-nasal (Na., $n = 3$), and ALI-polyp samples (Po., $n = 4$). miRNA expression counts were normalized using edgeR and $\log_2$ transformed for easier visualization. Circular expression heatmaps were plotted with the R ggplot2 package (red, low expression; green, high expression) for the most expressed miRNAs in ALI-bronchial cells (hsa-miR-92b-3p to hsa-miR-125a-5p). (C) Venn diagrams displaying the number of miRNAs significantly deregulated (edgeR algorithm, $p < 0.05$) in CF compared with NCF in ALI-nasal (Na.), ALI-bronchial (Br.), and ALI-polyp samples (Po.).

deregulated genes, *IGF1* and *WISP1* were predicted to be targeted by miR-181a-5p that was overexpressed in all three CF ALI-culture models. Moreover, a previous study reported that IGF1 is downregulated in CF [18], and WISP1 is a key protein in the wound healing mechanism [19] that includes the WNT pathway [20]. Based on these observations, we decided to ascertain the contribution of miR-181a-5p in *IGF1* and *WISP1* mRNA downregulation (Figure 2B, left bar charts). Our data showed that introduction of a miR-181a-5p inhibitor in CF ALI-bronchial cells led to an increase in *IGF1* and *WISP1* mRNA expression compared with the negative control, confirming that miR-181a-5p may play a role in their deregulation (Figure 2B, right bar charts).

IsomiR distribution in CF and NCF samples

We analyzed the isomiR distribution in CF and NCF ALI cultures ($n = 5$ each) to determine the extent of miRNA sequence variation and its possible biological implications (Figure 3A). As isomiRs are the results of combinations of different 5'- and 3'-ends of the canonical miRNA sequence, the observed frequency of individual ends was used to represent the isomiR distribution changes using sRNAbench. Analysis of the distribution of 329 expressed miRNAs revealed that the canonical sequence was the dominant isoforms (>50%) for about 46% of these miRNAs (Figure 3A) in CF and NCF ALI samples. The most common alteration in all ALI models was a change in the 3'-end position. Overall, sequence variations included nucleotide substitution (13.1%), 3'-extension (7.3%), 3'-trimming (19.7%), 5'-extension (0.8%), 5'-trimming (1.6%), and multiple variants (3.6%). Analysis of the relative expression [normalized using the Trimmed Mean of M-values (TMM) method] of the 30 most expressed miRNAs in NCF ALI-bronchial, ALI-nasal, and ALI-polyp samples indicated that for some miRNAs, such as miR-22, the canonical sequence (94% in all three models) was predominant (Figure 3B and supplementary material, Table S3). For about 16% of all miRNAs, the canonical form was detected in 80% of samples. Conversely, for some miRNAs (e.g. miRNA-141-3p, miR-30a/d/e, and miR-34b/c/449c), isomiR forms were predominant (supplementary material, Figure S2B). For instance, for miR-34b/c/449c, only 2% of sequences correspond to the canonical form, as previously published [21], and 61% of the detected forms had a divergent 5'-end with a modified 'seed' region compared with the reference sequence (supplementary material, Figure S2B). Moreover, analysis of the miR-101-3p variant sequence distribution showed differences between CF and NCF ALI-nasal samples. In NCF ALI-nasal samples, about 50% of all reads for miR-101-3p had a 5'-extension (divergent 5'-

Table 1. List of dysregulated miRNAs identified in ALI-bronchial cells CF versus NCF.

miRNA name	log FC	*p* EdgeR	*p* DeSeq
Up-regulated			
hsa-miR-138-5p	5.08	<0.0001	<0.0001
hsa-miR-4485-3p	2.69	<0.0001	<0.0001
hsa-miR-3065-3p	1.87	0.0001	0.0050
hsa-miR-1246	1.59	0.0272	NS
hsa-miR-449c-5p	1.48	0.0018	0.0193
hsa-miR-181b-5p	1.44	0.0001	0.0033
hsa-miR-449b-5p	1.31	0.0093	0.0342
hsa-miR-4532	1.19	0.0067	NS
hsa-miR-561-5p	1.00	0.0288	NS
hsa-miR-181a-5p	0.97	0.0006	0.0015
hsa-miR-181a-2-3p	0.94	0.0081	0.0422
hsa-miR-19b-3p	0.85	0.0299	NS
hsa-miR-181a-3p	0.85	0.0237	0.0424
hsa-miR-132-3p	0.80	0.0214	NS
hsa-miR-106b-3p	0.79	0.0116	NS
hsa-miR-92a-3p	0.74	0.0360	0.0470
hsa-miR-191-5p	0.72	0.0240	NS
hsa-miR-769-5p	0.72	0.0364	NS
Down-regulated			
hsa-miR-9-5p	−10.40	<0.0001	<0.0001
hsa-miR-127-3p	−3.00	<0.0001	NS
hsa-miR-10a-5p	−2.68	<0.0001	0.0288
hsa-miR-153-3p	−2.55	0.0004	0.0002
hsa-miR-362-5p	−2.19	0.0002	0.0005
hsa-miR-502-3p	−2.00	0.0021	0.0109
hsa-miR-203a-3p	−1.78	0.0452	NS
hsa-miR-501-3p	−1.77	0.0111	0.0016
hsa-miR-486-5p	−1.73	0.0267	NS
hsa-miR-152-5p	−1.61	0.0137	NS
hsa-miR-135b-5p	−1.41	0.0006	0.0032
hsa-miR-339-5p	−1.38	0.0029	0.0226
hsa-miR-654-3p	−1.38	0.0145	0.0440
hsa-miR-365a-3p/hsa-miR-365b-3p	−1.37	0.0020	0.0139
hsa-miR-500a-3p	−1.25	0.0006	0.0127
hsa-miR-532-3p	−1.18	0.0336	0.0294
hsa-miR-193b-3p	−0.92	0.0172	0.0361

miRNAs deregulated using the log FC and $p < 0.05$ identified as significantly deregulated by the EdgeR algorithm. DeSeq associated *P* values are also indicated when significant (NS, non-significant).
Log FC corresponds to the log of the ratio of miRNA level counts in ALI cells taken from five CF donors versus five healthy donors.

end) and about 50% had an unchanged 5'-end (Figure 3C). The canonical form represented 10.4% of total reads, and 26.2% of sequences had a 3'-extension and a conserved 5'-end. Among sequences with altered 'seed' due to a divergent 5'-end (5'-extension), there were sequences with an unchanged 3'-end (19.6%) or with 3'-trimming (23.5%), while the others showed 3'-extensions. The number of all miR-101-3p sequences with altered 'seed' sequence was significantly decreased by about 5% in CF nasal samples compared with NCF samples (Figure 3D). Overall, about 50% of miRNA sequences were divergent and 1.6% had a different 5'-end that could perturb the miRNA/mRNA interaction.

miR-101-3p and its isomiR expression and functional role

Previous studies showed that miR-101-3p is upregulated in lung disorders, including COPD [22], and is involved in *CFTR* mRNA regulation [14]. Moreover, *in silico* analysis of both *WISP1* and *IGF1* 3'-UTR regions predicted the presence of miR-101-3p recognition motifs. To assess the functionality of the major miR-101-3p isomiR, which probably results from a 1-nt shift of the DROSHA and DICER cleavage sites, oligonucleotides with 5'- or 3'-extensions were designed. IsomiR-101A, which corresponded to 18.5% of all sequences, was downregulated in CF ALI-nasal cells (−21%) and displayed a divergent 'seed' sequence with a 5'-extension and an unchanged 3'-end. Two other isoforms were studied, isomiR-101B (15.2% of all sequences and upregulated in CF ALI-bronchial cells, +23%) and isomiR-101C (5.9% of all sequences and upregulated in CF ALI-nasal cells, +35%) that displayed a 5'-end unchanged and a 3'-end with an extension (Figure 4A). The canonical miR-101-3p represented 9.5% of all sequences and was downregulated in CF ALI-nasal cells (−38%). The effect of the canonical miR-101-3p and isomiR variants on gene expression was then tested in BEAS-2B cells using a luciferase reporter assay under the control of the 3'-UTR of *CEBPA*, *EZH2* or *CFTR*, all three targeted by miR-101 (supplementary material,

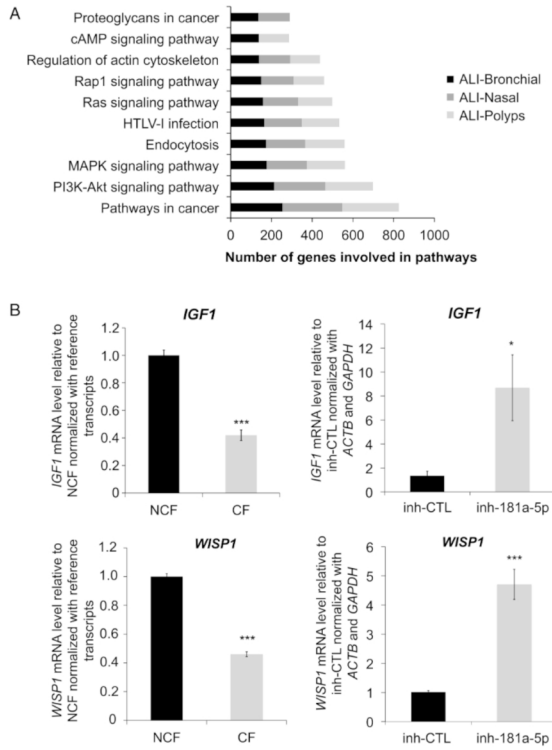

Figure 2. Genes and pathways targeted by deregulated miRNAs. (A) The ten pathways potentially most affected by the miRNAs deregulated in CF samples. Black bars: ALI-bronchial; dark grey bars: ALI-nasal; light grey bars: ALI-polyps. (B) Role of miR-181a-5p in *IGF1* and *WISP1* mRNA expression. Quantification of endogenous *IGF1* and *WISP1* mRNA levels in CF and NCF ALI-bronchial samples (left panels) and in CF ALI-bronchial cells after miR-181a-5p silencing or not (right panels). Mean + SEM. Welch's test, $^{*}p \leq 0.05$, $^{***}p \leq 0.001$.

Figure S3A,B). We focused on these genes as *EZH2* encodes a polycomb complex protein and is a well-known miR-101-3p target [23]. CEBPA is a key transcription factor in lung morphogenesis, and CFTR expression is regulated by miR-101-3p [14]. We showed that introduction of the canonical form of miR-101 induced a decrease in the luciferase level relative to *CEBPA*, *EZH2*, and *CFTR* 3'-UTR (Figure 4B). The isoforms 101A, 101B, and 101C had a repressive effect only on the 3'-UTR of *EZH2* and *CFTR* (Figure 4B). The effects of the canonical and isomiR miR-101-3p variants on *EZH2* and *CEBPA* mRNA expression were assessed in BEAS-2B cells. Canonical miR-101-3p reduced *EZH2* and *CEBPA* expression by 20–30% (Figure 4C), as we previously showed for *CFTR* [14]. The isomiR variants did not have any significant effect on *CEBPA* mRNA expression. Conversely, isomiR-101A negatively affected *EZH2* mRNA expression. Overexpression of each isoform was confirmed (Figure 4D). Analysis by western blotting for CFTR protein was carried out in 16HBE cells because of a weak expression in BEAS-2B cells, and the results showed that all isomiRs negatively affected the CFTR protein expression level (with a less pronounced effect with the canonical form) (Figure 4E). The isomiR variants also reduced EZH2 protein expression in BEAS-2B cells, in

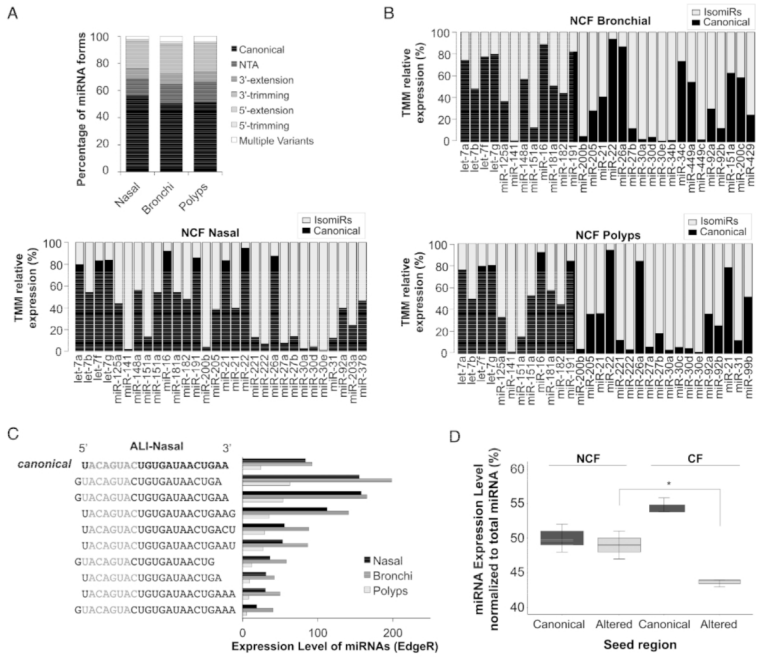

Figure 3. Expression levels of canonical miRNAs and isomiRs in NCF and CF samples. (A) Proportion of canonical miRNA and isomiR sequences annotated in NCF samples. Canonical forms reported in miRBase, nucleotide substitutions, and extension/trimming of 5'- or 3'-ends were plotted. IsomiR sequences containing multiple modifications were reported as multiple variants. (B) Distribution of the canonical and isomiR variants for the top 30 most expressed miRNAs in NCF ALI-bronchial, ALI-nasal and ALI-polyp cells. The percentage of total readcounts was plotted for each model. Black bars: canonical fraction (sequence similar to the miRBase entry); grey bars: isomiR fraction (including all modifications, 5'-, 3'-, and nucleotide variations). The miRNA strands detected are listed in supplementary material, Table S3. (C) Distribution of hsa-miR-101-3p canonical and isoform sequences (ten most represented variants in NCF ALI-nasal cells). The miRNA expression levels for each variant are represented in bar plots with normalized readcounts for the three *ex vivo* models. (D) Expression level of miR-101-3p variants containing the canonical or altered 'seed' in NCF and CF ALI-nasal samples. Boxplots were generated with the R package using edgeR-normalized readcounts ($n = 3$ per condition). Mean ± SEM, $^*p \leq 0.05$.

agreement with the luciferase assay and mRNA data for miR-101 and isomiR-101A, suggesting a cumulative impact of isoforms. Conversely, CEBPA protein expression was reduced only by isomiR-101A, and by isomiR-101B to a lesser extent, differently from the luciferase assay and mRNA results (Figure 4E). Taken together, these findings suggest that the effects of miR-101-3p and isomiR-101 change according to the target mRNA.

To further elucidate the function of miR-101-3p, bioinformatics tools were used to predict miR-101-3p targets. The WNT signaling pathway was among the top ten targeted pathways in the DAVID database. We silenced miR-101-3p in NCF human bronchial primary cells, and assessed the mRNA expression of genes related to the WNT signaling pathway using PCR array analysis with pre-designed primers. Silencing of miR-101-3p led to overexpression of mRNA for transcription factors such as paired-like homeodomain 2 (PITX2), growth factors such as IGF1, and WNT signal-transduction factors such as secreted frizzled related protein 2 (SFRP2) and WNT9A as well as WISP1 (Figure 4F).

miR-101-3p and miR-181a-5p influence the wound healing process

We sought roles for miR-101-3p and miR-181a-5p in regulation of *WISP1* expression, a key component of cell proliferation/migration programs. First we showed that

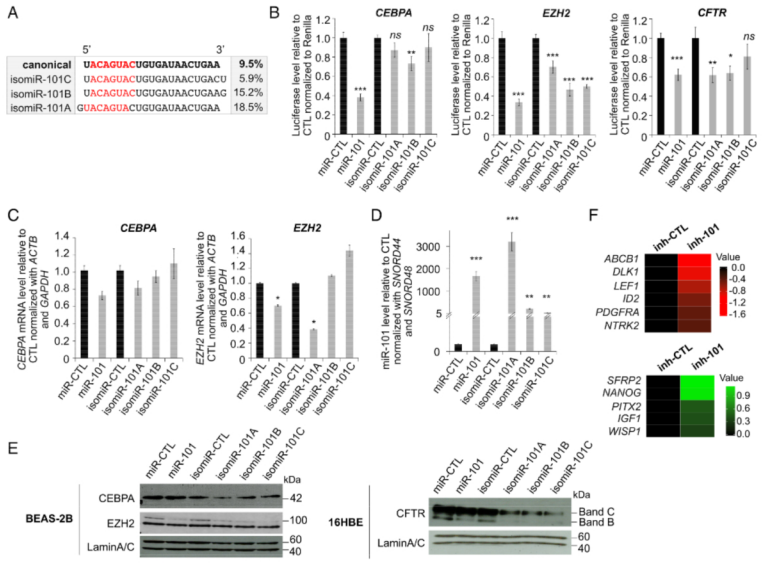

Figure 4. Role of miR-101-3p and isomiR. (A) Sequences and expression rate of the selected miR-101-3p variants (canonical and isomiRs). (B) The role of miR-101-3p (canonical sequence and isomiRs shown in A) were evaluated by luciferase activity of targeted genes in BEAS-2B cells. Mean ± SEM. *P* values were determined using the non-parametric Wilcoxon (unpaired) Mann–Whitney test. $^{*}p \leq 0.05$, $^{**}p \leq 0.01$, $^{***}p \leq 0.001$. (C) Effect of miR-101-3p and isomiRs on the expression of the indicated targeted genes was assessed using RT-qPCR in BEAS-2B cells. Data were normalized to the level of *ACTB* and *GAPDH* transcripts. Mean ± SEM. Welch's test, $^{*}p \leq 0.05$, $^{**}p \leq 0.01$, $^{***}p \leq 0.001$. (D) miR-101-3p and isomiR-101 expression levels assessed using RT-qPCR after transfection of the specific miRNA precursors or control in BEAS-2B cells. Data were compared with the expression of the internal controls *SNORD44* and *SNORD48* (small nuclear RNAs). (E) Effect of miR-101-3p and its variants on endogenous protein level in BEAS-2B and 16HBE cells for CFTR. Immunoblots were performed using anti-CEBPA (Abcam, 1:500), anti-EZH2 (Cell Signaling Technology, 1:1000), and anti-CFTR (Millipore, 1:200) antibodies (band B represents core glycosylated CFTR; band C represents the mature CFTR with complex glycosylation). Lamin A/C protein level (Cell Signaling Technology, 1:1000) was used as a loading control. (F) Effect of miR-101-3p silencing on the expression of genes involved in the WNT pathway. Heatmap represents quantification of endogenous mRNA levels in NCF human bronchial primary cells treated with inhibitor of miR-101-3p (inh-101) or control (inh-CTL). Only the significative deregulated genes are represented (Student's *t*-test processed according to Qiagen recommendations). Data were normalized to reference transcripts level (*ACTB, B2M, GAPDH, HPRT1, RPLP0*).

introduction of miR-101-3p and miR-181a-5p in bronchial cells induced a significant decrease in luciferase activity controlled by the 3'-UTR of *WISP1* (Figure 5A). Next we showed that silencing of miR-101-3p (which induces downregulation only for miR-101, isomiR-101B, and isomiR-101C; supplementary material, Figure 3C) and miR-181a-5p induced an increase in WISP1 expression in CFBE cells at both mRNA and protein levels (Figure 5B,C), where it is normally downregulated compared with 16HBE NCF cells (Figure 5D), data confirming the results obtained in CF ALI-bronchial samples (Figure 2B, lower right panel). Quantification of the levels of WISP1 by densitometry (at least three independent transfections) confirmed the increase in WISP1 expression after the inhibition of miR-101-3p and miR-181a-5p expression (Figure 5C, right panel). Silencing of miR-101-3p and miR-181a-5p was confirmed by RT-qPCR in CF cells (supplementary material, Figure 3D), although the miRNA amount quantified after transfection of its inhibitor should be considered with caution, due to potential limitations (inhibition through inhibitor/miRNA interaction without the miRNA degradation, interfering with PCR reaction) [24]. Similarly, miR-101-3p silencing induced an increase in WISP1 protein levels in non-CF bronchial cells, associated with an increase in β-catenin protein (Figure 5E), and in primary CF human bronchial primary cells (Figure 5F), which may play a role in driving

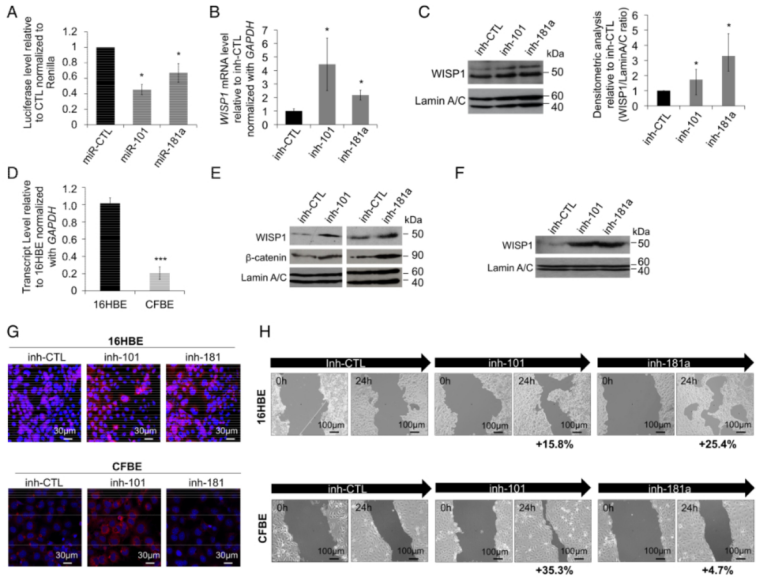

Figure 5. Impact of miR-101-3p and miR-181a-5p on WISP1 expression. (A) The impact of miR-101-3p or miR-181a-5p on the 3'-UTR-*WISP1* was evaluated using luciferase activity in BEAS-2B cells. Mean ± SEM. *P* values were determined using the non-parametric Wilcoxon (unpaired) Mann–Whitney test. *$p \leq 0.05$. (B) Quantification of endogenous *WISP1* mRNA levels in CFBE cells after silencing of miR-101-3p (inh-101) or miR-181a-5p (inh-181a) compared with the control (inh-CTL). Data were normalized to *GAPDH* transcript levels. Mean ± SEM. Welch's *t*-test, *$p \leq 0.05$. (C) Impact of miR-101-3p or miR-181a-5p silencing on the expression of WISP1 by western blotting in CFBE cells (left panel). Densitometric analysis of WISP1 protein band (western blotting) after miRNA silencing (shown in the left panel) in CFBE cells (right panel). Data were normalized to lamin A/C protein expression in each condition and are represented in normalized relative ratio. Mean ± SEM. Welch's *t*-test, *$p \leq 0.05$. (D) Quantification of endogenous *WISP1* mRNA levels in CFBE cells in comparison with 16HBE cells. Data were normalized to *GAPDH* transcript level. Mean ± SEM. Welch's test, ***$p \leq 0.001$. (E) Effect of miRNA silencing on the expression of WISP1 and β-catenin (differentiation marker) by western blotting in BEAS-2B cells. Mean ± SEM. Welch's test, ***$p \leq 0.001$. (F) Effect of miR-101-3p or miR-181a-5p silencing on the exprression of WISP1 protein in CF human bronchial primary cells (hAECB-CF). (G) 16HBE cells (top) and CFBE cells (bottom) were treated with inhibitor of miR-101-3p, miR-181a-5p or control for 24 h, then fixed and subjected to indirect immunofluorescence with anti-WISP1 antibodies. Cells were then stained with an Alexa-conjugated antibody (red). For nuclear staining, cells were counterstained with DAPI (blue). (H) Impact of silencing of miR-101-3p and miR-181a-5p on repair was observed in 16HBE and CFBE cells treated with inhibitor of miR-101-3p (inh-101), miR-181a-5p (inh-181a) or control (inh-CTL). Repair was measured 24 h after wounding and represented the mean of two independent experiments for 16HBE (4 or 5 areas per condition) and three independent experiments for CFBE cells (8–13 areas per condition). The percentage indicated corresponds to the wound repair rate compared with the control condition (inh-CTL).

the proliferative phase of wound healing, suggesting that the WISP1 inhibition observed in CF cells could be associated with impairment in cell repair. Immunofluorescence confirmed increased WISP1 levels after miR-101-3p and miR-181a-5p silencing, with the strongest effect for miR-101-3p (Figure 5G). Finally, increased wound healing was observed after miR-101-3p and miR-181a-5p silencing in monolayers of non-CF and CF cell lines (less marked with miR-181a silencing) (Figure 5H). These results suggest the importance of WISP1 expression, controlled by miR-101-3p and miR-181a-5p.

Discussion

The establishment of miRNA expression patterns with biological relevance remains challenging. Three main methods are used to quantify miRNA expression levels:

RT-qPCR [25,26], microarray hybridization [27,28], and massive parallel/next-generation sequencing (NGS) [29]. Although NGS data can be influenced by sequencing errors, this technology has accelerated the discovery of new miRNAs as well as sequence modifications in existing miRNAs, reflecting subtle variations in the landscape of mature miRNA sequences.

Here, we generated and compared the complete miRNA expression profiles of three *ex vivo* models of CF epithelium (polyps, nasal and bronchial cells from patients with the same genetic background: homozygous for the p.Phe508del *CFTR* mutation), and also identified novel miRNAs, including isomiRs, deregulated in CF. Comparison of the miRNA expression profiles in CF and NCF samples revealed that five miRNAs are dysregulated in all three *ex vivo* CF models compared with NCF controls. Our analysis indicated that miR-9-5p expression was strongly decreased in CF ALI-bronchial and CF ALI-nasal cultures compared with NCF ALI cultures, differently from a recent study showing miR-9 upregulation in CFBE41o$^-$ bronchial epithelial cell lines [30]. This miRNA is considered to have an anti-fibrotic role because of its reduced response to H_2O_2, and because many genes involved in the TGF-β pathway are its predicted targets [31]. NF-κB, a transcriptional factor that regulates a battery of genes and that is critical to innate and adaptive immunity, is upregulated in CF [32] and a well-described target for miR-9 [33]. Other miRNAs that were previously found to be upregulated in CF cultures showed similar expression in our CF and NCF cultures, for instance miR-138-5p [34]. It was previously reported that miR-138-5p enhances CFTR biogenesis and partially rescues p.Phe508-del-CFTR function in CF airway epithelia [34].

By using computational tools, we focused on gene targets belonging to the PI3K–Akt pathway, involved in cell proliferation, apoptosis, migration, and invasion, and to the wound healing signaling cascade that is perturbed in CF [35]. Indeed, recurrent infections and the associated inflammation in CF airways lead to a cycle of damage and repair of the epithelium surface [36,37]. As the estimates of false positives for conserved sites of some programs are close to 50% [38], it was crucial to functionally confirm the role on the predicted gene targets by using miRNA inhibitors. We found that silencing of miR-181a-5p (a miRNA that was upregulated in all three CF models) induced a marked increase in *WISP1* and *IGF1* mRNA expression in CF ALI-bronchial cultures. NGS also allowed evaluation of the distribution of miRNA variants, called isomiRs in NCF and CF samples. Comparison of all miR-101-3p sequences in ALI-nasal cultures showed that the isoform distribution was altered in CF samples compared with healthy controls. Moreover, for miR-449c, a member of the miR-449 family that are key factors required for motile ciliogenesis [39], isomiR variants represented the main sequences, as recently reported [21]. We then assessed the effect of miR-101-3p canonical and variant sequences on the expression/function of some of its targets. Previous studies showed that miR-101, which is evolutionarily conserved in vertebrates, controls *CFTR* mRNA stability in CF [14], in smoking-induced experimental conditions [40], and in other pulmonary diseases such as chronic obstructive pulmonary disease [41]. Variations in miRNA sequences can potentially affect the targetable genes/pathways due to an alternative choice between canonical and non-canonical 'seed' and/or by a 3'-compensatory interaction. The rules of target recognition by miRNAs are still not fully understood. Moreover, the identification of miRNA isoforms complicates the prediction of gene targets because the bioinformatics programs used are often based on canonical, i.e. referenced, miRNAs. Therefore, predictions remain uncertain and require experimental confirmation. As mRNA targets, we chose EZH2, which belongs to the polycomb group proteins, which are epigenetic regulators with an essential role in development through the deposit of repressive marks to maintain tissue-specific gene expression into adulthood [42]. Galvis *et al* demonstrated that EZH2 loss in lung epithelium leads to defective lung development. Indeed, EZH2 controls basal cell fate determination in embryonic lung endoderm, partly through repression of IGF1 expression [43]. Interestingly, potential miR-101-3p recognition motifs have been detected on *IGF1* and *WISP1* mRNA sequences. Inhibition of miR-101-3p expression in ALI-bronchial and ALI-nasal cells induced an increase in the *IGF1* and *WISP1* mRNA expression level. WISP1 (CCN4), like other members of the CCN family, is considered a matricellular protein that operates essentially in the extracellular microenvironment between cells, but with intracellular roles [44]. We finally demonstrated that the increase in WISP1 protein expression level induced by miR-101-3p and miR-181a-5p silencing is associated with a significant increase in wound closure in non-CF and CF cells.

In conclusion, our deep sequencing analysis of the miRNA profiles in CF and NCF ALI cultures of airway epithelium indicated that the expression of 15–27% of miRNAs is altered in CF samples, with variations also in isomiR distribution. Moreover, functional analysis showed that miR-181a-5p and miR-101-3p repress WISP1 expression in bronchial epithelial cell lines and ALI cultures of airway epithelium, and that miR-101-3p and miR-181a-5p silencing are associated with the concomitant rescue of WISP1 and β-catenin expression. Our findings suggest that deregulated miRNA expression may contribute to the outcomes of epithelial integrity loss in CF airway epithelium. Our complete analysis of miRNA expression patterns in CF ALI airway epithelia brings new insights into CF physiopathology and identified new candidates, WISP1 and/or miR-101, miR-181a, that could be further investigated as therapeutic targets.

Acknowledgements

This work was supported by grants from the French association Vaincre La Mucoviscidose (RF20150501432,

RIF20160501701, RIF20170502058) and FEDER-FSE-IEJ 2014/2020 (MTC). AP was supported by a PhD studentship from Vaincre La Mucoviscidose and AFM Téléthon (MTC). We also acknowledge the Respiratory Health Network of Québec (for the support of the Respiratory Tissue and Cell Biobank CRCHUM) and the Canadian Institutes of Health Research (CIHR, project grant PJT148593 to EB).

Author contributions statement

AP, SB, JV and KD performed most of the experiments with AP, who carried out mainly the luciferase and RNA analysis. SB participated in the luciferase assays, KD the western blotting, and JV the sequencing including the data analysis and wound healing assays. JB contributed to the molecular experiments using hAECB-CF. EB and AB provided ALI-polyp and ALI-nasal samples, respectively. MK and MC contributed substantially to revision of the manuscript. MTC initiated and managed the entire project.

Data availability statement

RNAseq files have been deposited in GEO (series accession number GSE159708); https://www.ncbi.nlm.nih.gov/geo/query/acc.cgi?acc=GSE159708.

References

1. Oglesby IK, Chotirmall SH, McElvaney NG, *et al*. Regulation of cystic fibrosis transmembrane conductance regulator by microRNA-145, -223, and -494 is altered in ΔF508 cystic fibrosis airway epithelium. *J Immunol* 2013; **190:** 3354–3362.
2. Oglesby IK, Agrawal R, Mall MA, *et al*. miRNA-221 is elevated in cystic fibrosis airway epithelial cells and regulates expression of ATF6. *Mol Cell Pediatr* 2015; **2:** 1.
3. Grimson A, Srivastava M, Fahey B, *et al*. Early origins and evolution of microRNAs and Piwi-interacting RNAs in animals. *Nature* 2008; **455:** 1193–1197.
4. Grimson A, Farh KK-H, Johnston WK, *et al*. MicroRNA targeting specificity in mammals: determinants beyond seed pairing. *Mol Cell* 2007; **27:** 91–105.
5. Guo L, Chen F. A challenge for miRNA: multiple isomiRs in miRNAomics. *Gene* 2014; **544:** 1–7.
6. Guo L, Lu Z. Global expression analysis of miRNA gene cluster and family based on isomiRs from deep sequencing data. *Comput Biol Chem* 2010; **34:** 165–171.
7. Lee LW, Zhang S, Etheridge A, *et al*. Complexity of the microRNA repertoire revealed by next-generation sequencing. *RNA* 2010; **16:** 2170–2180.
8. Neilsen CT, Goodall GJ, Bracken CP. IsomiRs – the overlooked repertoire in the dynamic microRNAome. *Trends Genet* 2012; **28:** 544–549.
9. Bhattacharyya S, Balakathiresan NS, Dalgard C, *et al*. Elevated miR-155 promotes inflammation in cystic fibrosis by driving hyperexpression of interleukin-8. *J Biol Chem* 2011; **286:** 11604–11615.
10. Oglesby IK, Bray IM, Chotirmall SH, *et al*. miR-126 is downregulated in cystic fibrosis airway epithelial cells and regulates TOM1 expression. *J Immunol* 2010; **184:** 1702–1709.
11. Ramachandran S, Karp PH, Osterhaus SR, *et al*. Post-transcriptional regulation of cystic fibrosis transmembrane conductance regulator expression and function by microRNAs. *Am J Respir Cell Mol Biol* 2013; **49:** 544–551.
12. Trinh NTN, Bilodeau C, Maillé É, *et al*. Deleterious impact of *Pseudomonas aeruginosa* on cystic fibrosis transmembrane conductance regulator function and rescue in airway epithelial cells. *Eur Respir J* 2015; **45:** 1590–1602.
13. Zhang P-X, Cheng J, Zou S, *et al*. Pharmacological modulation of the AKT/microRNA-199a-5p/CAV1 pathway ameliorates cystic fibrosis lung hyper-inflammation. *Nat Commun* 2015; **6:** 6221.
14. Viart V, Bergougnoux A, Bonini J, *et al*. Transcription factors and miRNAs that regulate fetal to adult CFTR expression change are new targets for cystic fibrosis. *Eur Respir J* 2015; **45:** 116–128.
15. Adam D, Bilodeau C, Sognigbé L, *et al*. CFTR rescue with VX-809 and VX-770 favors the repair of primary airway epithelial cell cultures from patients with class II mutations in the presence of *Pseudomonas aeruginosa* exoproducts. *J Cyst Fibros* 2018; **17:** 705–714.
16. Barturen G, Rueda A, Hamberg M, *et al*. sRNAbench: profiling of small RNAs and its sequence variants in single or multi-species high-throughput experiments. *Methods Next Generation Seq* 2014; **1:** 21–31.
17. Seyednasrollah F, Laiho A, Elo LL. Comparison of software packages for detecting differential expression in RNA-seq studies. *Brief Bioinform* 2015; **16:** 59–70.
18. Rogan MP, Reznikov LR, Pezzulo AA, *et al*. Pigs and humans with cystic fibrosis have reduced insulin-like growth factor 1 (IGF1) levels at birth. *Proc Natl Acad Sci U S A* 2010; **107:** 20571–20575.
19. Ono M, Masaki A, Maeda A, *et al*. CCN4/WISP1 controls cutaneous wound healing by modulating proliferation, migration and ECM expression in dermal fibroblasts via α5β1 and TNFα. *Matrix Biol* 2018; **68–69:** 533–546.
20. Whyte JL, Smith AA, Helms JA. Wnt signaling and injury repair. *Cold Spring Harb Perspect Biol* 2012; **4:** a008078.
21. Mercey O, Popa A, Cavard A, *et al*. Characterizing isomiR variants within the microRNA-34/449 family. *FEBS Lett* 2017; **591:** 693–705.
22. Ezzie ME, Crawford M, Cho J-H, *et al*. Gene expression networks in COPD: microRNA and mRNA regulation. *Thorax* 2012; **67:** 122–131.
23. Llorens F, Bañez-Coronel M, Pantano L, *et al*. A highly expressed miR-101 isomiR is a functional silencing small RNA. *BMC Genomics* 2013; **14:** 104.
24. Thomson DW, Bracken CP, Szubert JM, *et al*. On measuring miRNAs after transient transfection of mimics or antisense inhibitors. *PLoS One* 2013; **8:** e55214.
25. Chen C, Ridzon DA, Broomer AJ, *et al*. Real-time quantification of microRNAs by stem-loop RT-PCR. *Nucleic Acids Res* 2005; **33:** e179.
26. Shi R, Chiang VL. Facile means for quantifying microRNA expression by real-time PCR. *Biotechniques* 2005; **39:** 519–525.
27. Li W, Ruan K. MicroRNA detection by microarray. *Anal Bioanal Chem* 2009; **394:** 1117–1124.
28. Yin JQ, Zhao RC, Morris KV. Profiling microRNA expression with microarrays. *Trends Biotechnol* 2008; **26:** 70–76.
29. Hafner M, Landgraf P, Ludwig J, *et al*. Identification of microRNAs and other small regulatory RNAs using cDNA library sequencing. *Methods* 2008; **44:** 3–12.
30. Sonneville F, Ruffin M, Coraux C, *et al*. MicroRNA-9 downregulates the ANO1 chloride channel and contributes to cystic fibrosis lung pathology. *Nat Commun* 2017; **8:** 710.
31. Fierro-Fernández M, Miguel V, Lamas S. Role of redoximiRs in fibrogenesis. *Redox Biol* 2016; **7:** 58–67.

32. Bodas M, Vij N. The NF-κB signaling in cystic fibrosis lung disease: pathophysiology and therapeutic potential. *Discov Med* 2010; **9:** 346–356.
33. Wan H-Y, Guo L-M, Liu T, *et al*. Regulation of the transcription factor NI²-κB1 by microRNA-9 in human gastric adenocarcinoma. *Mol Cancer* 2010; **9:** 16.
34. Ramachandran S, Karp PH, Jiang P, *et al*. A microRNA network regulates expression and biosynthesis of wild-type and ΔF508 mutant cystic fibrosis transmembrane conductance regulator. *Proc Natl Acad Sci U S A* 2012; **109:** 13362–13367.
35. Trinh NTN, Bardou O, Privé A, *et al*. Improvement of defective cystic fibrosis airway epithelial wound repair after CFTR rescue. *Eur Respir J* 2012; **40:** 1390–1400.
36. Chmiel JF, Davis PB. State of the art: why do the lungs of patients with cystic fibrosis become infected and why can't they clear the infection? *Respir Res* 2003; **4:** 8.
37. Voynow JA, Fischer BM, Roberts BC, *et al*. Basal-like cells constitute the proliferating cell population in cystic fibrosis airways. *Am J Respir Crit Care Med* 2005; **172:** 1013–1018.
38. Pinzón N, Li B, Martinez L, *et al*. microRNA target prediction programs predict many false positives. *Genome Res* 2017; **27:** 234–245.
39. Marcet B, Chevalier B, Coraux C, *et al*. MicroRNA-based silencing of Delta/Notch signaling promotes multiple cilia formation. *Cell Cycle* 2011; **10:** 2858–2864.
40. Hassan F, Nuovo GJ, Crawford M, *et al*. MiR-101 and miR-144 regulate the expression of the CFTR chloride channel in the lung. *PLoS One* 2012; **7:** e50837.
41. Salimian J, Mirzaei H, Moridikia A, *et al*. Chronic obstructive pulmonary disease: microRNAs and exosomes as new diagnostic and therapeutic biomarkers. *J Res Med Sci* 2018; **23:** 27.
42. Boyer LA, Plath K, Zeitlinger J, *et al*. Polycomb complexes repress developmental regulators in murine embryonic stem cells. *Nature* 2006; **441:** 349–353.
43. Galvis LA, Holik AZ, Short KM, *et al*. Repression of Igf1 expression by Ezh2 prevents basal cell differentiation in the developing lung. *Development* 2015; **142:** 1458–1469.
44. Yeger H, Perbal B. CCN family of proteins: critical modulators of the tumor cell microenvironment. *J Cell Commun Signal* 2016; **10:** 229–240.